Naval Research Laboratory

Washington, DC 20375-5000

(2)

DTIC FILE COPY

NRL Memorandum Report 6677

AD-A226 443

NRL 1989 Beam Propagation Studies in Support of the ATA Multi-Pulse Propagation Experiment

RICHARD F. HUBBARD, A. WAHAB ALI, JAY P. BORIS,* PAUL BORIS,**
RICHARD F. FERNSLER, GLENN JOYCE, ELAINE ORAN,* J. MICHAEL PICONE*
STEVEN P. SLINKER AND RONALD D. TAYLOR†

Plasma Physics Division

**Laboratory for Computational Physics and Fluid Dynamics*

***SAIC, McLean, VA*

†Berkeley Research Associates, Springfield, VA

DTIC
ELECTE
SEP 13 1990
S D
D

August 31, 1990

Approved for public release; distribution unlimited.

REPORT DOCUMENTATION PAGE

Form Approved
OMB No. 0704-0188

Public reporting burden for this collection of information is estimated to average 1 hour per response, including the time for reviewing instructions, searching existing data sources, gathering and maintaining the data needed, and completing and reviewing the collection of information. Send comments regarding this burden estimate or any other aspect of this collection of information, including suggestions for reducing this burden, to Washington Headquarters Services, Directorate for Information Operations and Reports, 1215 Jefferson Davis Highway, Suite 1204, Arlington, VA 22202-4302, and to the Office of Management and Budget, Paperwork Reduction Project (0704-0188), Washington, DC 20503.

1. AGENCY USE ONLY (Leave blank)	2. REPORT DATE	3. REPORT TYPE AND DATES COVERED
	1990 August 31	Interim

4. TITLE AND SUBTITLE
NRL 1989 Beam Propagation Studies in Support of the ATA Multi-Pulse Propagation Experiment

5. FUNDING NUMBERS
JO #47-0900-0-0
ARPA Order #4395, A86

6. AUTHOR(S)
Richard F. Hubbard, A. Wahab Ali, Jay P. Boris,* Paul Boris,**
Richard F. Fernsler, Glenn Joyce, Elaine Oran,* J. Michael Picone,*
Steven P. Slinker and Ronald D. Taylor†

7. PERFORMING ORGANIZATION NAME(S) AND ADDRESS(ES)
Naval Research Laboratory
Washington, DC 20375-5000

8. PERFORMING ORGANIZATION REPORT NUMBER
NRL Memorandum Report 6677

9. SPONSORING/MONITORING AGENCY NAME(S) AND ADDRESS(ES)
DARPA
Arlington, VA 22209

NSWC
Silver Spring, MD 20903-5000

10. SPONSORING/MONITORING AGENCY REPORT NUMBER

11. SUPPLEMENTARY NOTES
*Laboratory for Computational Physics and Fluid Dynamics
**SAIC, McLean, VA
†Berkeley Research Associates, Springfield, VA

12a. DISTRIBUTION/AVAILABILITY STATEMENT
Approved for public release; distribution unlimited.

12b. DISTRIBUTION CODE

13. ABSTRACT *(Maximum 200 words)*

NRL theoretical and computational studies in support of the ATA Multi-Pulse Propagation Experiment (MPPE) are summarized in a series of papers which were presented at the 1989 Annual DARPA/SDIO/Services Charged Particle Beam Review. The six papers presented here were all written prior to the completion of the experiment. The first of these papers presents simulation results which modeled beam stability and channel evolution for an entire five pulse burst. The second paper describes a new air chemistry model used in the SARLAC propagation code and discusses the role of CO_2 in speeding channel heating. An overview of NRL studies on beam propagation in reduced-density channels is provided in the next paper. The fourth paper describes hydrodynamic simulations of convective mixing in beam-generated channels using a new flux-corrected transport algorithm developed for NRL's Connection Machine. The relative importance of high frequency (BBU-generated) and low frequency perturbations in triggering resistive hose instability is treated in the fifth paper, using results from the SARLAC beam simulation code. Finally, the last paper describes the various options for conditioning the ATA beam prior to injection into the propagation tank and concludes that a passive ion-focused regime (IFR) will produce the desired tailoring results.

14. SUBJECT TERMS		15. NUMBER OF PAGES
hose instability	beam propagation	41
~~ATA~~	charged particle beams	16. PRICE CODE
electron beams	air chemistry	

17. SECURITY CLASSIFICATION OF REPORT	18. SECURITY CLASSIFICATION OF THIS PAGE	19. SECURITY CLASSIFICATION OF ABSTRACT	20. LIMITATION OF ABSTRACT
Unclassified	Unclassified	Unclassified	SAR

CONTENTS

Accesion For
NTIS CRA&I
DTIC TAB
Unanno ced
Justificat
By
Distribution /
Availability Codes
Dist | Avail and / or Special
A-1

NRL 1989 BEAM PROPAGATION STUDIES IN SUPPORT OF THE ATA MULTI-PULSE PROPAGATION EXPERIMENT

OVERVIEW

This report contains six short papers which will appear in the proceedings of the 1989 Annual DARPA/SDIO/Services Charged Particle Beam Review which took place at the Naval Postgraduate School in Monterey, CA during 18-21 September, 1989. The report describes electron beam propagation and beam conditioning studies which have been carried out at NRL in support of the ATA Multi-Pulse Propagation Experiment (ATA/MPPE). These papers were all written prior to the actual propagation experiments which took place at the Lawrence Livermore National Laboratory during December, 1989 and January, 1990. Analyses of the experimental results will appear in the 1990 annual review.

ATA/MPPE was the first serious attempt to study the physics of beam propagation in the low density channel produced by a train or burst of pulses. The target beam parameters were 6 kA beam current, 10 MeV energy, 0.5 cm beam radius, 30 nsec pulse length, and 5 pulses separated by 1.2 msec. The two major experimental objectives were to investigate beam stability in a beam-produced channel to determine if the channel destabilized the beam and to demonstrate that subsequent pulses could travel farther than the first pulse ("range extension"). The papers presented here focused heavily on those objectives. It was recognized from the outset that the virulent resistive hose instability could disrupt the beam and prevent a range extension demonstration, and much of the experimental and theoretical effort concentrated on various beam conditioning techniques for suppressing that instability. In spite of these efforts, hose instability usually disrupted propagation during the first three meters of propagation.

A brief summary of each paper and a list of coauthors for each are given below. Papers on NRL theoretical studies of other CPB experiments will be published elsewhere.

A. Beam Stability and Range Extension Predictions for the ATA Multi-Pulse Propagation Experiment: Numerous simulations of the MPPE were undertaken. These simulations used the SIMMO particle simulation code for beam propagation during the pulse and the CHMAIR and HINT channel physics codes to treat the longer time scale behavior between successive pulses. For 6 kA, 5 mm, 33 nsec beams, range extension can be shown by about a 50%

Manuscript approved May 21, 1990.

increase in transported charge within 1 cm of the axis between the 1st and 5th pulses. The propagation range was 6 m. Channel depth is very sensitive to the amount of cooling present, ranging from around 1/4 ambient at the nozzle with no cooling to 1/2 with modest cooling. Four-to-one tailoring is sufficient for stable propagation to 6 m, if the initial offsets are under 0.1 mm. Hose displacement appeared to be more sensitive to initial displacement than to the presence of the channel. (Slinker, Hubbard, Ali, Fernsler, Joyce)

B. Air Chemistry Aspects of the ATA Multi-Pulse Experiment: A new air chemistry model for use in the propagation codes simulating the MPPE was developed by making analytic fits to benchmark runs with CHMAIR II. Range extension predictions were found to be not sensitive to the chemistry model. Beam stability was slightly worse. The use of CO_2 in the propagation chamber was also studied. It helps quench vibrational excitation of N_2, thereby opening the channel sooner. Although range extension can be seen without adding CO_2, its use, in small concentrations (~1%), is warranted. (SLinker, Ali)

C. Beam Propagation in Channels: This paper contains an overview of NRL research on propagation in channels and provides a brief summary of most of the other papers included in this report. Most of the work has been in support of the ATA Multi-Pulse Propagation Experiment (MPPE). Included are hose instability simulations, detailed air chemistry and channel physics calculations of ATA/MPPE. Simulation studies of SuperIBEX, PULSERAD and RADLAC propagation experiments are also briefly discussed. (Hubbard. Slinker, Taylor, Fernsler, Ali, Joyce, Boris)

D. Hydrodynamic Simulations of Beam-Generated Turbulence in Channels: A major uncertainty in the range extension simulations described in Section A above is the degree of convective mixing in the channel during the five pulse burst. To study this problem, we have developed a 2-D hydrodynamic simulation code which runs on NRL's new massively-parallel Connection Machine. The approach is the same as in the original Picone-Boris channel turbulence studies, but the simulations for MPPE parameters involve much longer time scales and require a finer mesh. Preliminary results indicate that the choice of a low value for the phenomenological convective mixing form factor used in the axisymmetric range extension simulations by Slinker, et al. is reasonable. (P. Boris, J. Boris, Hubbard, Oran, Picone, Slinker)

E. Sensitivity of Hose Instability to Frequency of Initial Perturbations in Low and High Current Beams: Increases in the solenoidal guide field B_z used in the ATA accelerator tend to reduce the growth of high-frequency BBU growth in the accelerator but enhance the generation of low-frequency sweep within the pulse. Hose instability in the propagating beam arises from initial perturbations generated by BBU and/or sweep. To examine the trade-offs between these two effects, a series of SARLAC simulations of ATA/MPPE were performed with an 830 MHz BBU-like perturbation in the x-direction and a simple linear sweep in the y-direction. The relative amplitudes of these perturbations were estimated from analytical models. In all cases, the BBU-like perturbations grew more rapidly as the beam propagated in air and eventually dominated even when suppressed by a 3 kilogauss guide field. One encouraging result was that sweep amplitudes much larger than the 0.01 cm design target for ATA/MPPE could apparently be tolerated. The results strongly suggest that suppression of BBU growth will be an important operational consideration. Similar simulations were carried out for the higher current RADLAC parameter regime; these simulations also showed that high frequency perturbations were more dangerous. One should be aware that high frequency perturbations within the beam lead to low frequency oscillations in z because the perturbations couple to hose in the beam head where the dipole decay length is short but the betatron wavelength is long. (Hubbard, Slinker, Taylor)

F. Beam Conditioning Options for the ATA Multi-Pulse Experiment: Stable propagation of the ATA/MPPE beam in air will require a head-to-tail emittance variation. Three strategies have been considered for introducing this variation: a multi-foil cell, a passive IFR cell and a differential focusing cell. All three have been analyzed using analytical models and axisymmetric FRIEZR simulations, and all are capable in principle of producing substantial emittance tailoring. The multi-foil cell, however, will probably scatter the beam too much and produces a less favorable tailoring profile. The passive IFR cell appears to produce the best results, especially when operated at low gas pressures. The differential focusing cell requires careful tuning, but it offers considerable flexibility and is the most compatible with the sweep-correcting FCC system. Current plans call for using the differential focusing cell with IFR as a backup. (Hubbard, Slinker, Fernsler, Joyce, Ali)

BEAM STABILITY AND RANGE EXTENSION PREDICTIONS FOR THE ATA MULTI-PULSE PROPAGATION EXPERIMENT*

S. Slinker, R. Hubbard, A.W. Ali, R. Fernsler and G. Joyce
Plasma Physics Division
Naval Research Laboratory

R.D. Taylor
Berkeley Research Associates

P. Boris
Science Applications Int. Corp.

Introduction. This paper summarizes our predictions for the ATA MPPE. For the nominal parameters, I_b = 6 kA, r_b = 0.5 cm, τ_p = 33 ns, N_p = 5 pulses, we predict that range extension can be shown by charge collection diagnostics at propagation distances of 3-6 meters into full density dry air. Longer propagation distances were not analyzed. For maximum initial hose perturbations under 0.1 mm, hose amplification of under 70 is seen for 6 meters of propagation. Stability, measured as an offset at a fixed laboratory position, is comparable for the first and fifth pulses. A 4 to 1 emittance tailoring over 12 ns was assumed. It also appears that hose displacement, at least for moderate propagation distances, is determined more by the initial perturbation than by the channel.

Other papers[1-3] in these proceedings discuss various aspects of this experiment.

Simulation Model. Several codes, which have been developed over the years, were combined to model this problem. Propagation was done with the particle simulation codes SIMMO, for axisymmetric cases, or SARLAC, for non-axisymmetric studies. These codes dumped the beam current density at specified propagation distances. For SARLAC, the current density was symmetrized because the hydro models were one-dimensional. The current density and channel profile were input to the detailed air chemistry code CHMAIR II. This code calculates the beam deposition, population of species, and channel temperatures but does not assume hydrodynamic expansion. CHMAIR II simulated about 100 ns, enough time for ohmic deposition to finish and for the electron and vibrational temperatures to equilibrate. The particle densities are then

consolidated and used as input to HINT. HINT is a one-dimensional hydro code which calculates the channel for the rest of the interpulse time (~1ms). The channel for the next pulse is then input to the propagation code and the process repeats for the next pulse. HINT has a simplified air chemistry model which includes 7 species and the gas and vibrational temperatures. It has cooling by thermal conduction, but not by radiation. Non-axisymmetric cooling is modeled by the Picone-Boris[4] theory. The fields are assumed to have decayed away.

Axisymmetric Studies. The following table summarizes the results of six axisymmetric simulations of the MPPE:

5 PULSE AXISYMMETRIC PROPAGATION RESULTS

Case	Chem.	Enhanced Cool. (f)	Enhanced Vib. Rel.	ρ_{min} z=0m	ρ_{min} z=4m	Q_1	Q_5
A	Old	0.0	No	.25	.64	11.0	20.4
B	Old	0.05	No	.53	.73	11.0	18.5
J	New	0.0	No	.26	.80	12.5	18.0
K	New	0.0	Yes	.25	.66	12.5	21.4
KM	New	0.05	Yes	.53	.74	12.5	18.9
KL	New	0.05	Yes	.55	.80	12.1	17.2

For Cases A and B the pulse separation was 1 ms; for the other cases it was 1.25 ms. In Case KL the nominal beam radius was 0.6 cm. The "Old" air chemistry is the standard VIPER model. The "New" air chemisty was obtained by benchmarking MPPE-type beams with the detailed air chemistry code CHMAIR II.[2] The enhanced cooling factor f is the phenomenological form factor in the Picone-Boris cooling theory which models non-axisymmetry hydrodynamic effects by using an enhanced thermal diffusivity.[3] "Enhanced Vibrational Relaxation" means the inclusion of carbon dioxide in the propagation chamber to thermalize the vibrational energy of nitrogen to aid hole boring.[2] ρ_{min} is the minimum fractional density at the entrance of the fifth pulse. Q_1 and Q_5 are the transported charges (μc) for pulses 1 and 5 within 1.125 cm of the

chamber axis at a propagation distance of z=6 m. Six meters is roughly twice the Nordsieck length of the initial pulse.

By comparing columns 7 and 8, all of these cases show at least an almost 50% increase in transported charge clearly verifying range extension.

Cases A and J differ in two ways: pulse separation time and air chemistry model. Case A shows slightly better range extension properties, particularly in channel depth at large propagation ranges. Its shorter pulse separation time allowed less thermal cooling, but the major reason for the deeper channel is a 15% greater direct deposition rate used with the "old" chemistry.

Non-axisymmetric hydrodynamic effects are modeled by using an enhanced thermal conduction

$$\lambda_T = \rho c_p c_s^2 \tau \frac{1}{4\pi} \ln\left[\frac{\rho_\infty}{\rho_0}\right] f, \qquad \text{ergs/cm-sec-}^\circ\text{K},$$

where τ is the pressure equilibration time and f is a form factor.[3,4] We have chosen f = 0.05 assuming an individual pulse has a symmetric deposition and the offsets between pulses are small compared to a beam radius. Cases A and B and Cases K and KM differ only in the value of f. A large difference in channel depth at the nozzle is shown even for f = 0.05. The channels with the nonzero f are slightly broader. At 4 m, the contrast is not as great. Charge transported 6 m is 10-15% lower with enhanced cooling but it is still appreciably higher for the fifth pulse than the first one. The amount of cooling is difficult to predict and the MPPE results will be very valuable.

The only difference between Cases J and K is the addition of carbon dioxide in the propagation chamber to aid in the thermalization of the vibrational energy of nitrogen. The channels at the nozzle at the entrance of the fifth pulse are very similar although the Case K channel opened much sooner[2]. At larger propagation distances Case K is definitely better and 15% better transport to 6 m is predicted. The use of carbon dioxide is recommended, though levels should be kept as low as possible, say ~ 1%, to avoid other air chemistry effects.

Cases KL and KM differ only in the nominal beam radius, which was 0.5 cm for KM and 0.6 cm for KL. The broader beam showed only slightly worse range extension at 6 m.

Non-axisymmetric Studies. Three of the non-axisymmetric simulations will be discussed here. The first modeled the beam into ambient air. The other two considered the fifth pulse: in one simulation the beam was injected into the (axisymmetric) channel of Case KM and the other into the deeper channel of Case K. The initial maximum perturbation was 0.1 mm in the x or y direction with the standard form. Sensitivity to the exact form of the initial perturbation is discussed in Reference 1. The following table shows the total charge and deposition centroids for several propagation distances.

	CHARGE CENTROID						DEPOSITION CENTROID					
	PULSE 1		PULSE 5-KM		PULSE 5-K		PULSE 1		PULSE 5-KM		PULSE 5-K	
Z(M)	X(CM)	Y(CM)	X	Y	X	Y	X	Y	X	Y	X	Y
1	.03	.03	.03	.04	.04	.05	.03	.04	.03	.04	.03	.04
2	-.12	-.10	-.15	-.15	-.16	-.17	-.13	-.12	-.16	-.16	-.15	-.16
3	-.10	-.15	-.03	-.10	.00	-.06	-.10	-.16	-.02	-.11	.00	-.06
4	.10	.04	.20	.15	.25	.20	.11	.04	.21	.16	.23	.19
5	.28	.25	.28	.28	.22	.36	.30	.27	.29	.30	.21	.33
6	.15	.19	-.06	-.06	-.06	-.23	.16	.20	-.07	-.07	-.07	-.21

Through 5 m the centroids of all three pulses track each other to within a millimeter. This indicates that the hose displacement is determined more by the initial perturbation than by the presence of the channel. Thus, employing a moveable charge collection diagnostic to catch the hosing beams may be successful. The maximum offset of any beam slice in the beam body is around 0.5-0.7 cm for all three cases over the 6 m range.

Conclusions. If the design parameters are met, the MPPE should be successful. The beam will be stable enough to travel over 6 m and dig enough of a channel to show range extension. Beam stability will not be very sensitive to the channel. The greatest unknown will be the effect of anomalous cooling.

References.

1. R.F. Hubbard, et al., "Sensitivity of Hose Instability to Frequency of Initial Perturbations in Low and High Current Beams", these proceedings.
2. S. Slinker, et al., "Air Chemistry Aspects of the ATA Multipulse Experiment", these proceedings.
3. P. Boris, et al.,"Hydrodynamic Simulations of Beam-Generated Turbulence in Channels", these proceedings.
4. J.M. Picone and J.P. Boris, Phys. Fluids 26 365-382 (1983); J.M. Picone, et al., "PHAZR: A Phenomenological Code for Holeboring in Air", NRL Memo Rpt. 5647 (1985).

*Work supported by the Defense Advanced Research Projects Agency, ARPA Order No. 4395, Amendment 80, monitored by the Naval Surface Warfare Center.

Air Chemistry Aspects of the ATA Multipulse Experiment*

S. Slinker and A.W. Ali
Plasma Physics Division
Naval Research Laboratory

R.D. Taylor
Berkeley Research Associates

Introduction. Two studies involving air chemistry aspects of the MPPE are discussed in this paper. The first study develops a simple air chemistry model, appropriate for the conditions encountered in the MPPE, which was incorporated in the propagation codes SIMMO and SARLAC. The second study considers the use of carbon dioxide in the experimental tank to help relax the beam-pumped vibrational excitation energy of nitrogen in order to aid channel formation. How the results of these studies affect the predictions for the MPPE are discussed elsewhere in these proceedings.[1]

Air chemistry model. The air chemistry relevant to intense beam propagation and channel formation is quite complex and can be sensitive to reaction rates. Air chemistry codes involving many species and reactions have been written which describe the situation in great detail. However, these models are much too expensive computationally to be directly coupled to a propagation code and so simplified air chemistry models need to be written. An equation for electron production is used which has bulk coefficients for the various processes. These coefficients are functions of the reduced electric field only. They are found from benchmark runs with the detailed air chemistry code CHMAIR II.

The propagation code model equations for the electron production and conductivity are

$$\frac{dn_e}{dt} = \frac{1}{\Delta W}\frac{d\varepsilon}{dx}\frac{J_b}{e}P + \alpha(\xi)n_e P - \beta(\xi)n_e^2 - \chi(\xi)n_e P^2 \ ,$$

and

$$\sigma = \frac{e^2}{m}\frac{n_e}{\nu_m(\xi)P + \nu_{ei}(n_e,T_e)} \ ,$$

where n_e is the electron density, σ is the conductivity, $\Delta W \sim 34$ eV/ion-pair, $d\varepsilon/dx \sim 2500$ eV/cm, J_b is the beam current density, P is the

*Work supported by the Defense Advanced Research Projects Agency, ARPA Order No. 4395, Amendment No. 80, monitored by the Naval Surface Warfare Center.

fractional background density and ν_{ei} is the electron-ion collision frequency. The bulk coefficients are the avalanche coefficient α, the recombination coefficient β, the attachment coefficent χ, the electron-neutral collision frequency ν_m and the electron temperature T_e. These are all functions of $\xi \equiv E/N$, the electric field over the particle density.

The five bulk coefficient functions are obtained from fitting data from a 4 pulse MPPE holeboring run with CHMAIR II. The data were taken at 0,2,4 and 6 m from the nozzle and at 14 radial points, 0 to 2.5 cm from the axis. The simple two parameter fitting form A exp (Bξ) was chosen. There is no fundamental reason for choosing this form other than simplicity. In practice, rather than calculate the chemistry coefficients on the run, the propagation codes create tables of the coefficients indexed by the reduced electric field and then do fast table lookups.

PROPAGATION AIR CHEMISTRY USED FOR THE MPPE SIMULATIONS

COEF.	A	B	RANGE	COEF.	A	B	RANGE
α	2.73×10^{-9}	1.32	$0\le\xi\le11.19$	ν_m	5.82×10^{11}	.1234	$0\le\xi\le3.02$
	1.54×10^{-5}	.548	$11.19\le\xi\le30$		7.66×10^{11}	.0327	$3.02\le\xi\le12.99$
	1.78×10^{-2}	.3129	$30\le\xi\le65$		8.85×10^{11}	.0215	$12.99\le\xi$
	8.02×10^{3}	.1126	$65\le\xi\le200$	T_e	.187	.1233	$0\le\xi\le3.69$
β	1.45×10^{-7}	-.234	$0\le\xi\le4.93$		.255	.0389	$3.69\le\xi\le13.88$
	4.87×10^{-8}	-.0124	$4.93\le\xi$		.306	.0257	$13.88\le\xi$
χ	3.75×10^{7}	-.159	$0\le\xi\le6.49$				
	1.78×10^{7}	-.044	$6.49\le\xi$				

(ξ is measured in Townsends: 1 Td = 10^{-17} v-cm^2 = 246 v/cm @ 1 atm.)

Several differences with the "VIPER" air chemistry model which has been our standard propagation model can be noted. Attachment was not in the VIPER chemistry. The avalanche ionization coefficient is much higher here at low values of ξ. This is because there is considerable nitrogen oxide (~10^{16}) in the channel and it is easier to ionize than N_2 or O_2. Nevertheless, avalanche ionization is a very small effect for MPPE parameters. Because of clusters the bulk recombination coefficient is larger than the VIPER value. No systematic study has been made to show the effect of the chemistry model change on beam stability predictions. The initial pulse into ambient air shows the hose growth to be slightly larger with the new chemistry. Range extension predictions are not altered.[1]

Vibrational Relaxation of Nitrogen. Considerable beam-deposited energy can be tied up in the vibrational excitation of nitrogen. The relaxation time, which depends on the gas and vibrational temperatures and the composition, can be quite long (>ms). If that energy could be released rapidly into thermal energy, hole boring would be faster. One technique for doing this is to add a buffer gas which has the property that it quenches the vibrational excitation. Two candidates are water vapor and carbon dioxide. Both of these are present in ambient air. Because water vapor enhances cluster formation and attachment, possibly affecting beam stability, carbon dioxide should be a better first choice. McDonnell-Douglas has shown experimentally that the addition of carbon dioxide can aid in channel formation and a simple analysis by Ali et al.[2] has shown this to be the case.

The following rates (cm^3/sec) are used to relax the vibrational energy: $8.5x10^{-7}exp(-12.06/T_g^{1/3})$ for collisions with N_2 and O_2, $1.07x10^{-10}exp(-3.18/T_g^{1/3})$ for collisions with O, $6x10^{-13}$ for collisions[3] with CO_2 and $3.1x10^{-15}$ for collisions with H_2O.

Two MMPE runs were made to illustrate the effect of carbon dioxide in the propagation chamber. CASE J had an initial background of 80% nitrogen and 20% oxygen. CASE K had 80% nitrogen, 20% oxygen and 0.03% carbon dioxide (=$7.4x10^{15}$ /cc). This is about the normal carbon dioxide particle density in ambient air. With the rate quoted this gives a relaxation time of ~ 0.2 ms. The dissociation fraction of the carbon dioxide was assumed to be the same as that of nitrogen and oxygen and the density was proportional to the local density. No other chemistry effects of carbon dioxide were included.

The graph shows the channel conditions at propagation distances of z = 0,2,4 and 6 m at the entrance of the fifth pulse. At the nozzle the channels with and without carbon dioxide are similar. This is because the temperature has been raised enough and there is sufficient atomic oxygen around that the other channels for vibrational relaxation are open. Nevertheless, the hole at the nozzle was opened quicker in the carbon-dioxide-aided case. At greater propagation distances the channel is clearly deeper for CASE K.

Charge transport results predict that either case will show range extension. However, the addition of carbon dioxide to the propagation chamber is probably worth the effort. Bieniosek (private communication)

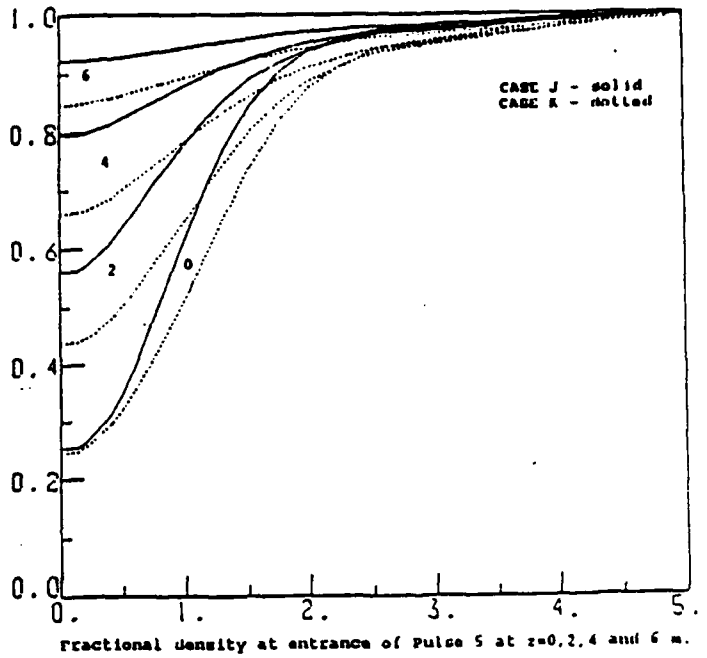

was not able to see channel enhancement until the fraction of carbon dioxide was around 1% or greater, and he found the best effect was with 6%. This may indicate that the rate quoted above was too high or else the efficiency for transfer of the excited carbon dioxide energy to heat is less than expected. A few percent of carbon dioxide may not alter the air chemistry much, however, carbon dioxide has a momentum transfer cross section $\geq$ 10 times that of nitrogen at electron energies $<$ 0.2 eV and also it decreases as the electron energy increases. These complications suggest using the minimum amount having the desired effect. However, a detailed analysis of energy exchange and radiation from CO_2 is required for a comprehensive understanding of the role of CO_2 in hole boring.

References.

1. S. Slinker, et al., "Beam Stability and Range Extension Predictions For the ATA Multi-Pulse Propagation Experiment", these proceedings.
2. A.W. Ali, et al., these proceedings (1987).
3. R.L. Taylor and S. Biberman, Rev. of Mod. Phys., 41 26-47 (1969).

BEAM PROPAGATION IN CHANNELS*

R. F. Hubbard, S. P. Slinker, R. D. Taylor,** R. F. Fernsler
A. W. Ali, G. Joyce and P. Boris***
Plasma Physics Division, Naval Research Laboratory, Washington, DC 20375

I. INTRODUCTION

Beam propagation in density channels is a major focus of the current DARPA experimental program. The ATA Multi-Pulse Propagation Experiment (MPPE) will attempt to demonstrate stability, tracking, and range extension in the channel formed by a five-pulse burst of 10 MeV, 6-8 kA beams. Also, tracking experiments at NRL using the PULSERAD and SuperIBEX beams in laser-guided electric discharge (LGED) channels are in progress. This paper provides an overview of theoretical work at NRL in support of these propagation experiments. More detail can be found in Refs. 1-7.

II. ATA MULTI-PULSE PROPAGATION STUDIES

Overview: Detailed predictions for an ATA/MPPE burst require treatment of the complicated coupling between beam propagation and channel physics over times scales up to 5 msec. To address these problems, we have carried out five-pulse axisymmetric simulations which combine existing NRL propagation and channel physics codes.[1] The results are used to predict the range of each pulse and to provide realistic channels for SARLAC hose stability simulations. Supporting these simulations are more detailed studies of air chemistry effects[2] and convective cooling.[3] We have also studied the sensitivity of lead pulse hose instability growth to the amplitude of BBU and corkscrew-induced perturbations[4] and choice of emittance tailoring method.[5] We have assessed the feasibility of an ATA pulse-decoupling experiment.[6]

Typical parameters for these studies are beam energy E_0 = 10 MeV, peak current I_0 = 6 kA, nominal beam radius a_b = 0.5 cm. pulse length τ_p = 33 nsec, pulse separation τ_s = 1.25 msec, and an emittance variation of 4:1.

Multi-pulse axisymmetric propagation and channel dynamics:[1] In these simulations, the SIMMO particle code is used for $\tau < \tau_p$ to propagate the beam and dump beam current density $J_b(r,\zeta,z)$. Here, ζ is the distance from the

beam head, z is the propagation distance, and $\zeta = c\tau = ct - z$. CHMAIR II uses the J_b input from SIMMO to calculate beam and ohmic deposition and detailed air chemistry for $\tau_p < \tau < 2\tau_p$ at several z-locations. HINT is then used to calculate the long-time-scale behavior of the channel ($\tau < \tau_s$), including the effects of hydrodynamic expansion, thermal and convective cooling, and vibrational relaxation. This generates a density profile, $\rho(r,z)$, which is input into SIMMO for the next pulse in the burst, and the process is repeated.

Six simulations were run to determine the sensitivity of the channel depth and the transported beam fluence to model assumptions. The fluence, $Q_n(R,z)$, is defined as the transported beam charge for the n^{th} pulse within a radius, R, of the beam axis at a fixed location z. The ratio Q_5/Q_1 for R = 1.1 cm and z = 6 m varied between 1.4 and 1.85, indicating modest range extension. The channel depth at z = 0 was very sensitive to the assumed Picone-Boris form factor f for convective cooling;[3,8] the on-axis density at the fifth pulse was a factor of two higher when f was raised from 0 to 0.05. However, the predicted fluence at z = 6 m changed by less than 15% because the convectively-cooled channel was significantly broader. Changes in the assumed chemistry model for SIMMO and the inclusion of enhanced vibrational cooling from CO_2 produced only modest changes in the fluence.[2]

Chemistry effects and convective cooling in ATA/MPPE: A new chemistry model for SIMMO and SARLAC was developed using these same basic approach as in the standard "VIPER" model. The new model[2] includes attachment and revised rate coeficients benchmarked against detailed CHMAIR II calculations in the ATA/MPPE regime. The new model gives similar axisymmetric behavior and generates slightly more hose instability growth. The second major focus of the air chemistry studies was a treatment of the transfer of the energy stored in N_2 vibrational excitations to gas heating. This process occurs on the millisecond time scale but can be speeded up by adding a small amount of CO_2.

The Picone-Boris[8] convective cooling form factor, which we and others have used in MPPE hydro simulations is a phenomenological model which has not been benchmarked against full 2-D hydro code results in the appropriate parameter regime. A new 2-D hydro code that treats the convective cooling process directly has been developed.[3] The code runs on NRL's massively-parallel Connection Machine and is much faster than the version used by Picone and Boris. Preliminary results suggest that the value f = 0.05 used in the HINT code is reasonable for the level of asymmetry expected for ATA/MPPE.

Hose instability growth in MPPE: SARLAC simulations[1] have been carried out in the channels generated by the SIMMO-CHMAIR-HINT simulation sequence described above. Hose amplitudes in the beam body grow from an assumed initial level of 0.01 cm to 0.5-0.7 cm in 6 m of propagation. Similar hose amplitudes were observed in the absence of a channel.

Increasing the guide field B_z in ATA increases low frequency sweep displacements but suppresses high frequency BBU-induced perturbations.[4] The effect of this tradeoff on hose instability was investigated using SARLAC by initiating a BBU-like mode in x and a linear sweep in y. The BBU-induced mode was much more unstable in the simulations, while relatively large sweep amplitudes could be tolerated. In one set of SARLAC runs, increasing B_z from 1 to 3 kG caused hose amplitudes at $z = 6$ m to drop by almost a factor of 3.

Other SARLAC simulations considered the effects of different possible emittance tailoring techniques.[5] Beam radius and emittance profiles were generated by FRIEZR for various tailoring schemes, and the results were used to initialize SARLAC. A multi-foil tailoring cell simulation produced hose amplitudes in excess of 1 cm in 4.8 m of propagation, while a similar run using a 5 mtorr IFR cell grew to only 0.1 cm.

Pulse decoupling experiment for ATA:[6] SARLAC was used to investigate the feasibility of studying pulse decoupling experimentally on ATA by applying a weak deflecting guide field just before the last pulse. The simulation results suggest that the phenomenon would likely be obscured by wall forces.

Summary: The ATA/MPPE beams are likely to propagate with only moderate hose growth if the stringent beam conditioning goals are met. Range extension effects should be modest but observable.

III. SUPERIBEX AND PULSERAD TRACKING STUDIES

PULSERAD stability and tracking simulations:[7] A data base now exists for the 1988 NRL tracking experiments which used the 1 MeV PULSERAD beam. SARLAC simulations were performed with a weakly-tailored beam with the estimated experimental parameters. The hose amplitudes were somewhat higher in a centered density channel than in full density air, but the difference could be attributed entirely to scattering effects. Increasing I_0 appeared to destabilize the beam. The tracking distance was typically 30 cm. All of these results are consistent with the experimental data.

SuperIBEX stability and tracking simulations: SARLAC was used[7] to model the 4.5 MeV SuperIBEX tracking experiments currently in progress. The simulations assumed moderate emittance tailoring and relatively large amplitude, but low frequency initial hose perturbations. Peak simulation beam currents varied between 10 and 40 kA. Hose amplitudes increased with I_0 and were smaller in the presence of a channel than in full density air, in contrast to the PULSERAD result. Tracking distances were predicted to be only 20-30 cm in the presence of an offset channel.

A separate series of SARLAC simulations modeled propagation in a 10 m long tank in uniform 0.5 atm air and in a centered, 0.1 atm density channel. The beam was well-conditioned, as might be produced by a two-stage IFR/active-wire conditioning cell currently being considered for future experiments. The perturbations were the same as used in the RADLAC simulations described in Ref. 4. Hose amplitudes grew to only 0.2-0.3 cm in the SuperIBEX simulations.

Summary: PULSERAD simulation results were consistent with the data from the successful 1988 tracking experiment. Simulations of the current SuperIBEX tracking experiment predict short tracking distances and moderately-strong hose growth. Future SuperIBEX experiments with well-conditioned beams could exhibit "stable" propagation to ranges beyond 10 m.

IV. REFERENCES

1. S. Slinker et al., "Beam Stability and Range Extension Predictions for the ATA Multi-Pulse Experiment," these proceedings.
2. S. Slinker et al., "Air Chemistry Aspects of the ATA Multi-Pulse Experiment," these proceedings.
3. P. Boris et al., "Hydrodynamic Simulations of Beam-Generated Turbulence in Channels," these proceedings.
4. R. Hubbard et al., "Sensitivity of Hose Instability to Frequency of Initial Perturbations in Low and High Current Beams," these proceedings.
5. R. Hubbard et al., "Beam Conditioning Options for the ATA Multi-Pulse Experiment," these proceedings.
6. R. Fernsler et al., "Pulse Decoupling Using ATA," these proceedings.
7. R. Taylor et al., "Analysis of Channel Tracking in SuperIBEX and PULSERAD," these proceedings.
8. J. Picone and J. Boris, Phys. Fluids 26. 365 (1983).

*Supported by the Defense Advanced research Projects Agency, ARPA Order No. 4395, Amendment 80, Monitored by the Naval Surface Warfare Center,

**Berkeley Research Associates, Springfield. VA 22150

***Science Applications International Corp., McLean, VA 22102

HYDRODYNAMIC SIMULATIONS OF BEAM–GENERATED TURBULENCE IN CHANNELS*

P. Boris**, J. Boris, R. Hubbard, E. Oran, J. Picone, S. Slinker

Plasma Physics Division

Naval Research Laboratory, Washington, DC 20375–5000

INTRODUCTION

Heated columns or channels have been produced at several laboratories using lasers, guided discharges, or propagating relativistic electron beams. These experiments[1] have shown that turbulent or convective mixing of the hot air with the cooler gas outside the channel causes the channels to cool much more rapidly than expected from classical thermal conduction. Picone and Boris[2] modeled this process using a standard 2–D FCT hydro code and developed simple phenomenological models for incorporating convective cooling in axisymmetric models. These simple models use a form factor f to model the cooling process and have been used by several groups[3,4] to predict range extension effects in the upcoming ATA Multi–Pulse Propagation Experiment (ATA/MPPE).

ATA/MPPE will attempt to produce beams which can propagate with modest hose instability growth, thus producing nearly axisymmetrc deposition patterns. However, most previous experiments and simulations treated cases with highly asymmetric deposition profiles, so relatively little is known in the regime of interest to ATA/MPPE. In this paper, we describe 2–D hydro calculations using a new FCT[5] algorithm developed for NRL's massively–parallel Connection Machine. Since the time scales of interest for ATA/MPPE are much longer than those in the original Picone–Boris study[2] and a finer spatial grid is required, these simulations would have been very expensive to run on a CRAY. A major goal of this study is to estimate the scaling of the Picone–Boris form factor f in the nearly–axisymmetric regime.

PROBLEM DEFINITION

A version of the LCPFCT[6] code was run for several sets of possible ATA/MPPE parameters. Both two pulse and five pulse cases were studied. The turbulence problems were set up on a 256 by 256 grid with periodic boundary conditions. Both a stretching and a damping factor were added to the grid in order to limit errors caused by reflected shock waves feeding back into the calculations through the boundary conditions. The simulations assumed that the first pulse generated a smooth gaussian density depression, and the calculations began at the arrival of the second pulse, which created an offset gaussian overpressure. In the five pulse cases, a third pulse was added after 2.0 ms, a fourth after 4.0 ms, and so forth. Each pulse after the second was offset from the channel center randomly in a square pattern at a distance L, 0.5 cm in this case. The random placement of these pulses simulated the inherent uncertainty in aiming the particle beam in the experiment.

The physical parameters for the two pulse case were: characteristic channel radius, R_c = .800 cm, characteristic beam radius, R_b = .600 cm, channel center density, $\rho_c = 8.90 \times 10^{-4}$ gm/cc, and beam center overpressure, $\delta P_b = 2 \times P_a$. The numerical parameters were set to a cell size of 0.1 cm in both the x and y directions and to a simulation run time of 2.0 ms.

The multi–pulse case had these parameters: characteristic channel radius, $R_c = .888$ cm, characteristic beam radius, $R_b = .600$ cm, channel center density, $\rho_c = 5.90 \times 10^{-4}$ gm/cc, and beam center overpressure, $\delta P_b = 2 \times P_a$. The numerical parameters were set to a cell size of 0.1 cm in both the x and y directions and to a simulation run time of 6.8 ms.

DESCRIPTION OF CODE

Compressible gasdynamic problems generally involve both rotational effects (vortices, turbulence, etc.) and compressible effects (sound waves, shocks, etc.) but are described by a set of multidimensional continuity equations (partial differential equations) which express the physical laws of mass, momentum, and energy conservation. In 2–D gasdynamics there are four continuity equations all having basically the same form. Each of these equations requires an accurate, high-resolution algorithm for its solution because fluid problems generally generate very steep gradients in the solution such as at shocks and vortex interaction boundaries.[7]

Each of the four individual continuity equations, in each of the two Cartesian directions is solved by a single, highly optimized algorithm called Flux-Corrected Transport which guarantees the physically important positivity property of fluid mass and energy densities. This fluid convection module to solve the set of coupled continuity equations, is the most recent one-dimensional version of the FCT algorithm[5], LCPFCT. This flexible general module is used with direction and timestep splitting to construct two-dimensional simulations which allow physically realistic boundary conditions in a number of non-periodic geometries. The kernel of the algorithm consists of about 30 lines of C-star which has been specifically designed and optimized for parallel computation on the Connection Machine.

A Connection Machine consists of many thousands of individual scalar processors connected in a hypercube configuration[8]. Communication to and control of these processors is through a front-end computer. At NRL, there are two Connection Machines, one with 16,384 (16K) processors and one with 8,192 (8K) processors. The user controls these through one of several kinds of front ends: a VAX, a Symbolics, or a Sun. Each of the individual processors can be reconfigured into a larger number of virtual processors, typically in powers of two, the actual number limited by the storage required for the algorithm and the size of the computational grid. Floating-point arithmethic is carried out by Weitek chips, each of which does pipelined processing of the floating-point operations for 32 of the scalar processors.

RESULTS

In order to estimate the Picone–Boris form factor, f: the equation given by $f = \kappa / g(\delta P_b / P_a)(R_b^2/\tau_{eq}) ln(\rho_a/\rho_c)$ must be solved. Here, κ was the integrated vortex filament strength, $g = (R_{bf} - R_b)^2/R_b^2$ was a measure of the beam expansion rate to its final value R_{bf}, δP_b was the beam–generated overpressure, P_a was the ambient pressure, τ_{eq} was the equilibration time for the vortex filament strength, and ρ_a and ρ_c were the ambient and channel densities, respectively. For the parameters listed above, the quantity $g = 0.23$.

Values of f, κ, and τ_{eq} are listed in table 1 for various values of the beam–channel offset, L. Table 1, yielded the graph in figure 1 which represented one curve of the family of curves that make up the form factor. The curve obtained by this code strongly resembled the curves generated by Picone and Boris and for $L < R_b$, f was proportional to L, thus supporting the

assumptions made in Ref. 3.

The following pictures show graphically the turbulent effects that can occur with multiple particle beams in air. The first set of parameters was for a two pulse simulation and figures 2 and 3 show density contours and vorticity contours. The second set of parameters was for a five pulse case where figures 4 and 5 correspond to the same quantities as described in the two pulse case.

CONCLUSIONS

Figure 2 showed that over the 2 ms time scales of relevance for ATA/MPPE the channel did not deform significantly for the listed parameters. This figure, coupled with the lack of turbulence seen on the vorticity plot in figure 3 and with the velocity data taken from the FCT code (vmax after equilibrium of 2-3 meters/second) lead to the conclusion that turbulence won't be a factor in the two pulse experiments.

The five pulse case was very different, however. Figure 4 showed much greater channel deformation after the fifth pulse than was seen in the two pulse case. This deformation, added to the complex vorticity pattern shown in figure 5 and the large maximum fluid velocities (10-15 meters/second) lead to the conclusion that turbulence would play a major role in the beam propagation experiment modeled by this simulation. The turbulence effect could be lessened if the beam–channel offsets are kept small (i.e. less than $\approx 0.1\, R_b$) and interpulse separation short (i.e. less than ≈ 1 ms).

The beam–channel offset used for the five pulse simulations in this paper was probably too large for the ATA/MPPE experiment. The pulse to pulse overpressure ratio in the actual experiment will decrease with pulse number. As a result of these factors, more simulations will have to be conducted to better model the experiment.

REFERENCES

1. J.R. Greig, R.E. Pechacek, and M. Raleigh, Phys. Fluids 28, 2357 (1985).
2. J.M. Picone and J.P. Boris, Phys. Fluids 26 365–382 (1983).
3. S. Slinker et al, Poster I–27, these proceedings.
4. D. Keeley and D. Welch, (private communications).
5. J.P. Boris, and D.L. Book, Solution of the Continuity Equation by the Method of Flux-Corrected Transport, *Methods in Computational Physics*, 16, 85-129, 1976.
6. *LCPFCT – A Monotone Algorithm for Solving Continuity Equations*, J.P. Boris, J.H. Gardner, E.S. Oran, S. Zalesak, J. Ellzey, G. Patnaik, D.L. Book, R.H. Guirguis, to appear as a Naval Research Laboratory Memorandum Report, 1989.
7. *Fluid Dynamic Computations on a Connection Machine – Preliminary Timings and Complex Boundary Conditions*, E.S. Oran, J.P. Boris, P.R. Boris, E. Brown, and C. Li, Presentation & AIAA Paper 90–xxxx, AIAA 28th Aerospace Sciences Meeting, Reno NV, 8–11 January 1990.
8. *Connection Machine, Model CM-2 Technical Summary*, Thinking Machines Corporation, Cambridge, MA, 1989.

* Supported by the Defense Advanced Research Projects Agency, ARPA Order No. 4395, Amendment 80, monitored by the Naval Surface Warfare Center.

** Science Applications International Corp., Mclean, VA

Table 1: Form Factor Terms

L	κ	τ_{eq}	f
0.0	0.0 (cm^2/sec)	$\approx 90\ \mu s$	0.0
0.05	44.5 (cm^2/sec)	$\approx 90\ \mu s$	0.06
0.20	148.2 (cm^2/sec)	$\approx 90\ \mu s$	0.21
0.35	224.3 (cm^2/sec)	$\approx 100\ \mu s$	0.35
0.50	258.7 (cm^2/sec)	$\approx 110\ \mu s$	0.44
0.75	225.6 (cm^2/sec)	$\approx 110\ \mu s$	0.40
1.00	146.3 (cm^2/sec)	$\approx 120\ \mu s$	0.23
1.20	62.3 (cm^2/sec)	$\approx 120\ \mu s$	0.12

Fig. 1: Form Factor Curve

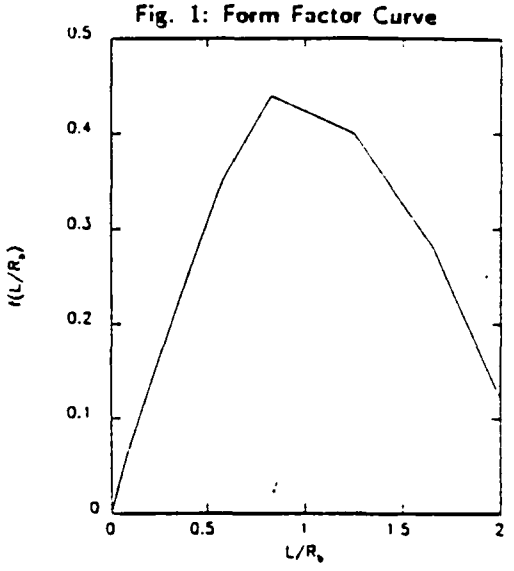

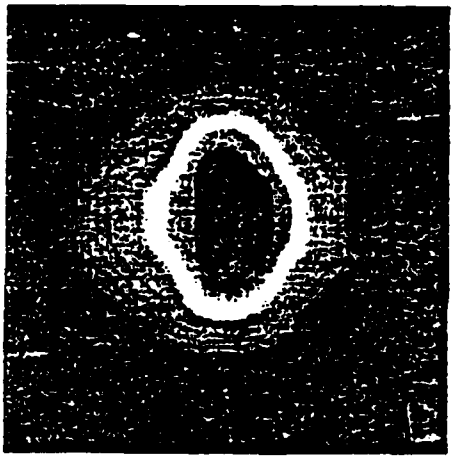

Fig. 2: Two–Pulse Density Contour

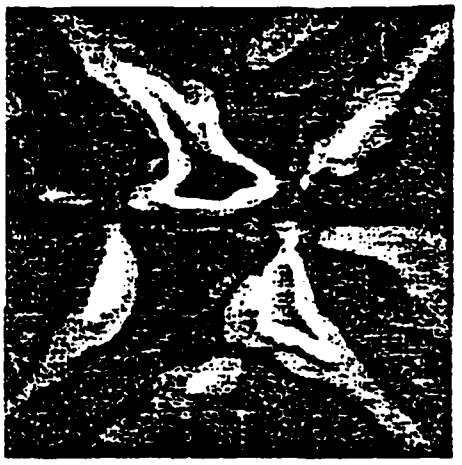

Fig. 3: Two–Pulse Vorticity Contour

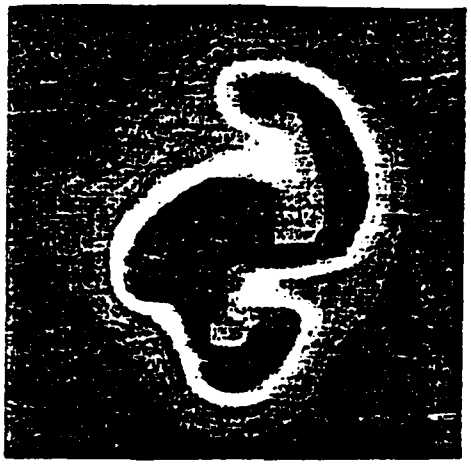

Fig. 4: Multi–Pulse Density Contour

Fig. 5: Multi–Pulse Vorticity Contour

SENSITIVITY OF HOSE INSTABILITY TO FREQUENCY OF INITIAL PERTURBATION IN LOW AND HIGH CURRENT BEAMS*

R. F. Hubbard, S. P. Slinker and R. D. Taylor**
Plasma Physics Division, Naval Research Laboratory, Washington, DC 20375

I. INTRODUCTION

Most studies of resistive hose instability in propagating electron beams have assumed that the frequency spectrum of the initial perturbation cannot be experimentally controlled. However, Fawley has pointed out that for the ATA Multi-Pulse Propagation Experiment (MPPE), the relative amplitudes of low frequency sweep and high frequency (BBU-induced) perturbations are sensitive to the guide field, B_z, in the accelerator. Increasing B_z reduces the growth of BBU but enhances corkscrew-induced sweep.

We have used the SARLAC hose instability code[1] to determine which class of perturbations is the more dangerous. SARLAC models beam propagation in the atmosphere using the doppler-shifted coordinates z and $\zeta = ct - z$. Here, z is the propagation distance in air and ζ is the distance from the beam head. A BBU-like 830 MHz perturbation, $X(\zeta,z=0)$, is imposed in the x-direction using an asymptotic BBU growth model from Caporaso.[2] A low frequency (LF) sweep perturbation is imposed in the y-direction. In general, the hose growth in the x-direction dominates even when its initial amplitude is substantially lower, suggesting that ATA should be operated with a high B_z. Similar results have been obtained by Feinstein and Keeley.[3] HF perturbations also generate more instability growth in RADLAC simulations. These HF perturbations initiate hose growth in the "neck" of the beam where the dipole decay length is relatively short. Since the local betatron wavelength is usually long in this region, an HF perturbation may generate <u>low</u> frequency oscillations in z.

II. ATA HOSE SIMULATIONS

<u>BBU perturbation model:</u> Following Caporaso,[2] the beam exits the accelerator with a displacement $X(\zeta,z=0) = X_0\exp(KNI_b(\zeta)Z_\perp\omega_0/B_z)\sin(\omega_0\zeta/c)$. Here, I_b is the beam current in kA, the cavity impedance $Z_\perp = 30\ \Omega$, $\omega_0/2\pi = 8.3\times10^8\ sec^{-1}$, the number of cavities $N = 50$, $B_z = 1\text{-}3$ kG, $X_0 = 10^{-4}$ cm and

the coefficient $K = 1.16 \times 10^{-13}$ kG-sec(kA-ohm)$^{-1}$. The beam is assumed to have an energy of 10 MeV with the current ramping to its nominal value $I_0 = 6$ or 8 kA over a distance $\zeta_r = 360$ cm. The injected radius and emittance profiles follow the form shown in Fig. 4 of Ref. 4 which are generated from a FRIEZR simulation of a 5 mtorr passive IFR conditioning cell.

Corkscrew or sweep perturbation model: Low frequency sweep or corkscrew arises from the coupling between energy variations $\Delta\gamma$ within the pulse and field or alignment errors. This produces a phase advance, $\delta\phi = (\Delta\gamma/\gamma)\int k_c dz$, where the cyclotron wavenumber k_c is proportional to B_z. For $\delta\phi << 1$, the phase advance and sweep amplitudes are proportional to B_z. In SARLAC, this effect is modeled by imposing an initial perturbation in the y-direction given by $Y(\zeta, z=0) = \alpha B_z \zeta$. The coefficient α is chosen to be 3×10^{-5} (kG)$^{-1}$.

Results: Four long SARLAC simulations were run with the parameters described above. Cases A1, A2 and A4 were for $I_0 = 6$ kA and $B_z = 1$, 1.5 and 3 kG, respectively, while Case A3 used an 8 kA beam with a 1.5 kG guide field. Results are summarized in the table below. The displacements X and Y are taken in the beam tail at $\zeta = 750$ cm (25 nsec) and are tabulated at injection ($z = 0$) and at $z = 5.4$ m.

Case	I_o	B_z	X(0)	Y(0)	X(5.4m)	Y(5.4m)
A1	6 kA	1.0 kG	0.010 cm	0.022 cm	0.31 cm	0.12 cm
A2	6	1.5	0.0035	0.034	0.20	0.12
A3	8	1.5	0.010	0.034	0.67	0.14
A4	6	3.0	0.0006	0.068	0.11	0.12

Figure 1 plots the initial perturbations $X(\zeta,0)$ and $Y(\zeta,0)$ for Case A2, showing that the HF perturbation (solid curve) is an order of magnitude lower than the sweep perturbation (dashed curve). However, Fig. 2 shows that at $z = 6$ m, the HF modes induced in the x-direction have surpassed those in the y-direction. Increasing I_0 to 8 kA results in a substantial increase in X, both because the BBU-induced initial perturbation is larger and because the higher current beam travels more betatron wavelengths. The resulting hose amplitudes are shown in Fig. 3. The results suggest that ATA should be operated with a relatively high guide field to suppress BBU and that relatively large sweep amplitudes may be tolerated without initiating serious instability growth.

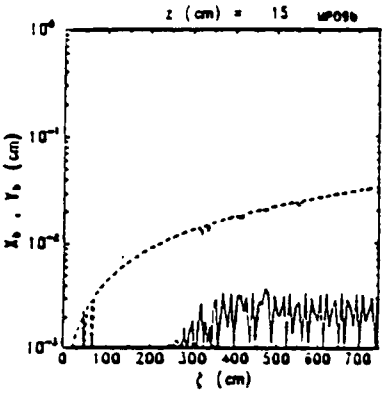

Fig 1. Initial displacement $X(\zeta,0)$ and $Y(\zeta,0)$ (solid and dashed lines): Case A2

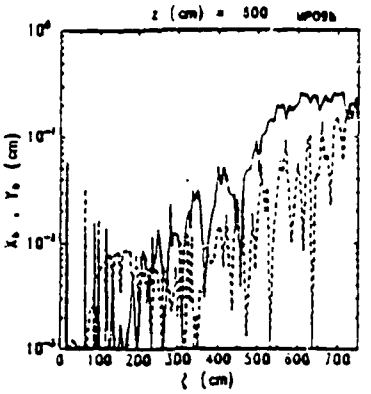

Fig 2. $X(\zeta)$ and $Y(\zeta)$ at $z = 6m$ for Case A2. BBU-induced hose is stronger (solid line).

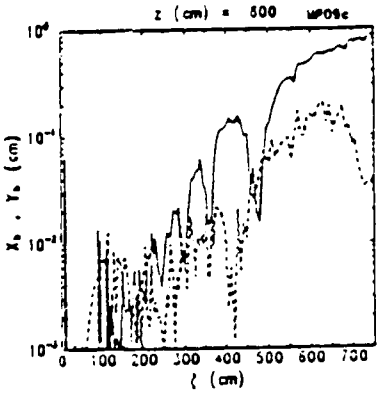

Fig 3. $X(\zeta)$ and $Y(\zeta)$ at $z = 8m$ or Case A3. I_0 is raised to 8 kA; beam is more unstable.

III. RADLAC HOSE INSTABILITY SIMULATIONS

Overview: Both HF and LF perturbations are produced in RADLAC even though BBU is thought to be unimportant. A series of SARLAC simulations were performed using a 0.02 cm, 830 MHz HF perturbation in x and a 0.2 cm (at ζ = 900 cm) sweep perturbation in y. Nominal beam parameters in the simulations were I_0 = 25 kA, γ_0 = 41 (ramped in some cases), beam radius a_b = 2 cm, rise length ζ_r = 300 cm and normalized emittance taper ε_t = 2-4.

RADLAC simulation results: Six simulations were performed as described in the table below. E_{min} and E_{max} define the range of the energy ramp, and X_{max} and Y_{max} are the maximum hose amplitudes at ζ = 900 cm and $z < 12$ m.

Case	E_{min}	E_{max}	η_t	Comment	X_{max}	Y_{max}
R1	20 MeV	20 MeV	4	-	0.5 cm	0.5 cm
R2	20	20	4	a_b=1.5cm	2.5	0.8
R3	5	20	2	-	> 20	> 5
R4	5	20	4	-	4.5	1.5
R5	5	20	4	Y_0=0.02cm	4.5	0.6
R6	10	20	4	Faster γ-ramp	1.1	0.4

As in the ATA simulations, the high frequency modes dominate even though they are initiated at a smaller amplitude. Comparing Cases R1 and R3, it is apparent that relying on the natural tailoring which comes about from the energy ramp may lead to unacceptably large hose amplitudes. This is, in part,

because the head is so hot that it is quickly lost, leaving behind a poorly-tailored beam. Even when the 4:1 emittance variation is restored to a beam with a γ-ramp (Case R4), the beam is more unstable than in the constant energy case. Figure 4 plots X(z) and Y(z) at ζ = 675 cm for Case R4, showing an initial damping of the LF mode followed by an eventual coupling to the faster-growing HF mode. Hose amplitudes versus ζ at z = 120 cm are shown for this case (Fig. 5) and for the more unstable weakly-tapered Case R3 (Fig. 6).

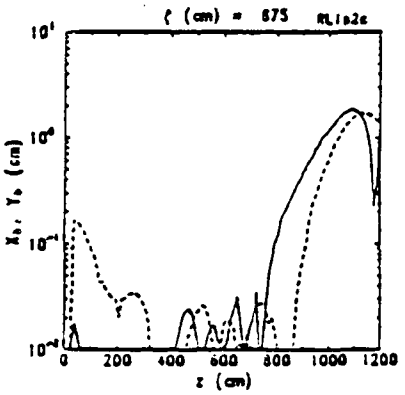

Fig 4 X(z) and Y(z) at ζ = 675cm for RADLAC Case R4. Note initial decay in Y (dash line).

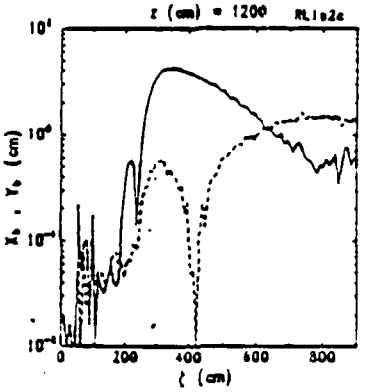

Fig 5. X(ζ) and Y(ζ) at z = 12 m for Case R4. HF mode (solid line) dominates.

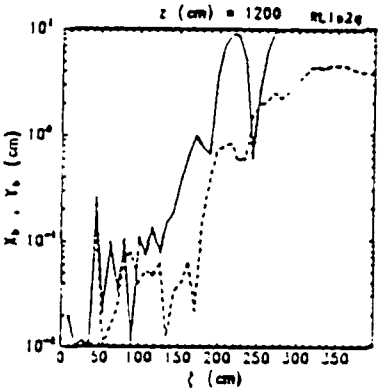

Fig. 6. X(ζ) and Y(ζ) at z = 12 m for Case R4 (weaker taper). Note shorter pulse length.

IV. CONCLUSIONS AND REFERENCES

For both ATA and RADLAC, high frequency perturbations appear to couple more strongly to the resistive hose instability and should be suppressed if possible even at the expense of higher sweep amplitudes.

1. G. Joyce, R. Hubbard, M. Lampe and S. Slinker, J. Comp. Phys. **81**, 193 (1989).
2. G. Caporaso, A. Cole and K. Struve, LLNL Report UCID-88262 (1983).
3. D. Keeley, "Hole Boring and Hose Instability Studies for ATA MULti-Pulse Experiment," these proceedings.
4. R. Hubbard et al, "Beam Conditioning Options for the ATA Multi-Pulse Expeiment," these proceedings.

*Supported by the Defense Advanced research Projects Agency, ARPA Order No. 4395, Amendment 80, Monitored by the Naval Surface Warfare Center,

**Berkeley Research Associates, Springfield, VA 22150

BEAM CONDITIONING OPTIONS FOR THE ATA MULTI-PULSE EXPERIMENT*

R. F. Hubbard, S. P. Slinker, R. F. Fernsler, G. Joyce and A. W. Ali
Plasma Physics Division, Naval Research Laboratory, Washington, DC 20375

I. INTRODUCTION

The ATA Multi-Pulse Propagation Experiment (MPPE) will be the first serious attempt to study beam stability, tracking and range extension for a WIPS-mode pulse train. The accelerator is expected to produce 5 beam pulses separated by 1.25 msec with peak current I_0 = 6-8 kA, radius a_0 = 0.5 cm and a nominal energy of 10 MeV. However, it is expected that the beam will be disrupted by the resistive hose instability unless a substantial head-to-tail variation in beam emittance is introduced.[1] This paper examines three emittance tailoring techniques which are currently being considered for ATA/MPPE: a multi-foil cell, a classical (passive) IFR cell and a differential focusing or energy variation system. All three techniques introduce a beam radius variation $a_b(\zeta)$ where $\zeta = ct - z$ is the distance from the beam head; the beam is then passed through a final scattering foil which converts much of this variation to a variation $\varepsilon_n(\zeta)$ in the normalized emittance. Our studies have primarily been performed using the FRIEZR axisymmetric simulation code.

II. MULTI-FOIL TAILORING CELLS

Description of technique: When a relativistic beam passes through a thin conducting foil, the radial electric field is shorted out, and the beam experiences a focusing force similar to that produced by a solenoidal magnetic lens.[2,3] The focal length f_L scales with $a_b\gamma/I_b$. Fawley[4] has proposed using three thin foils positioned so that the beam body ($I_b = I_0$) is focused to a small radius while the lower current beam head expands to a larger radius. Since γ is nearly constant in ATA, the radius profile $a_b(\zeta)$ arises from the rise in beam current $I_b(\zeta)$ in the beam head.

Modifications to FRIEZR simulation code: The FRIEZR code has been upgraded to include foil focusing, scattering, and solenoidal lenses. Foils and lenses may be located anywhere in the beamline. Foil focusing is treated using a thin lens approximation:[2,3] each beam electron is given an inward impulse with a focal length whose variation with r is shown in Fig. 1 of Ref. 3, assuming a Bessel beam profile. Foil scattering is treated by imparting an appropriate random kick to each simulation particle as it passes through the

foil. Solenoidal lenses are treated by specifying a focal length f_L at the lens location and adding an impulse $\delta p_x/p_z = -x/f_L$ and $\delta p_y/p_z = -y/f_L$.

Simulation results for multi-foil cell: A series of simulations were performed for a 6 kA, 10 MeV beam with an injection beam radius $a_b(0) = 0.8$ cm, wall radius b = 7 cm, beam rise length $\zeta_r = 360$ cm, initial normalized emittance $\varepsilon_n(0) = 0.5$ rad-cm and an upstream lens placed so that $da_b/dz = 0.03$ at the first foil. Carbon foils 2 mils thick were placed at z = 0, 39, and 50 cm with a thicker 30 mil foil at z = 78 cm. (Fawley suggested similar foil locations for a shorter three-foil cell). Figure 1 plots the half-current and rms beam radii (lower and upper curves, respectively) as functions of ζ at the final foil. The desired beam taper is produced with $a_{1/2}$ varying by a factor of 4.5. The corresponding emittance taper is shown in Fig. 2. At ζ = 600 cm, ε_n is almost a factor of four above its injection value. This is due primarily to scattering, but a portion arises from weak variations in focal length length contained in Eq. (1). The latter effect is proportional to $a_b\nu_b/\gamma$ and can result in huge emittance increases for high ν/γ beams such as SuperIBEX.

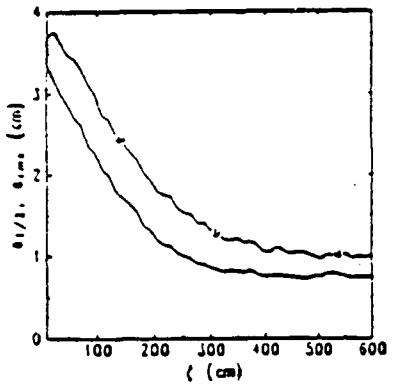

Fig 1. Beam $a_{1/2}$ and a_{rms} vs ζ at end of 78 cm long 2-2-2-30 mil carbon multi-foil cell.

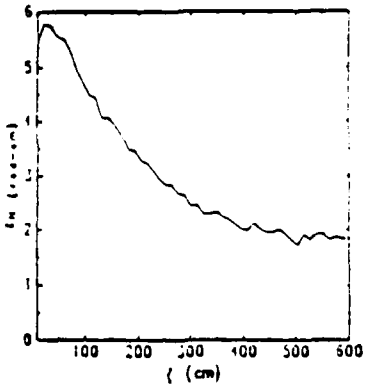

Fig 2. Emittance vs ζ for the cell used in Fig. 1. Location is just after final foil.

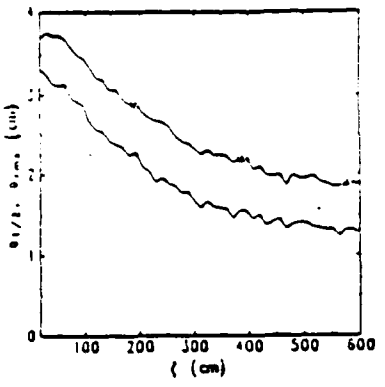

Fig 3. Beam $a_{1/2}$ and a_{rms} vs ζ at end of 78 cm long 5-5-5-30 mil carbon multi-foil cell.

When foil scattering is eliminated, the minimum half-current radius drops from 0.7 cm to 0.4 cm. However, even 2-mil foils are unlikely to survive multi-pulse ATA operation. When the first three foils are 5-mil, a_b rises to an unacceptable 1.3 cm, as shown in Fig. 3. Thus, foil scattering may severely limit the usefulness of this technique for ATA. Also, the relatively sharp radius taper in Fig. 1 is not favorable for hose stabilization.

III. PASSIVE IFR TAILORING CELL

Description of technique: Passive or classical IFR cells have been extensively used on ATA in the past to taper the beam. The beam is passed through a low pressure gas, producing a plasma column whose density, $n_i(\zeta)$, increases during the pulse. Provided $n_i < n_b$, the radial electric field produced by the beam density, n_b, expels plasma electrons, leaving behind an ion column which electrostatically pinches the beam. FRIEZR has been extensively used in the past to model such conditioning cells.[5]

IFR cells in multi-pulse operation: Although passive IFR cells have not been operated in a multi-pulse machine, we believe the beam will be tailored in the same manner as in single pulse operation. The dominant atomic physics process between pulses is expected to be charge exchange between fast ions and ambient neutral gas atoms or molecules. Hole boring should be insignificant because the collisional mean free paths are large at these gas densities. By the time the next pulse arrives, the plasma density is expected to be much to low to influence the beam. We believe that IFR cells on ATA have performed well, especially considering the inverse tailoring apparently produced by laser-ion guiding in the accelerator.

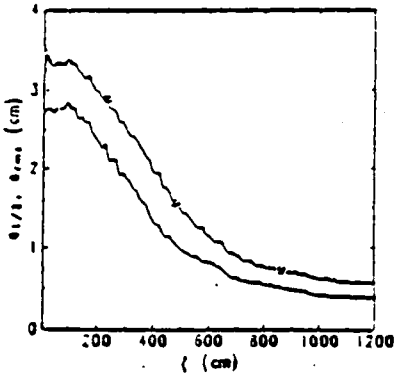

Fig 4. Beam $a_{1/2}$ and a_{rms} vs ζ at end of a 5 mtorr passive IFR cell.

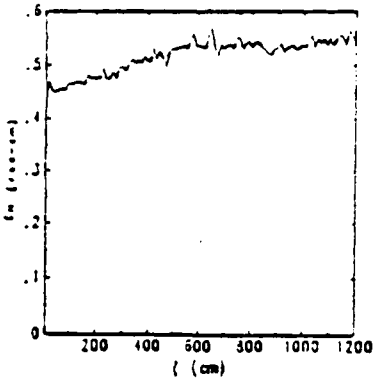

Fig 5. Beam emittance vs ζ just before final scattering foil for the IFR cell in Fig.4.

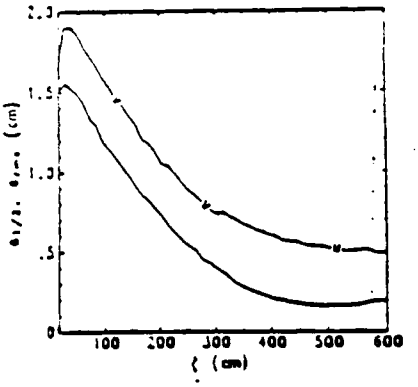

Fig. 6. Beam $a_{1/2}$ and a_{rms} for a differential focusing cell with a 20% energy variation.

Simulation results for a passive IFR cell: Although most experiments and simulations in the past have utilized IFR cell pressures of 20 mtorr or higher, lower pressures may be more effective if the beam emittance is not too large. Figure 4 plots $a_{1/2}(\zeta)$ and $a_{rms}(\zeta)$ at $z = 90$ cm for a beam similar to that described in the previous section. The gas was assumed to be air at 5

mtorr. Figure 5 plots $\varepsilon_n(\zeta)$ just before the exit foil, showing essentially no emittance growth from the injected value. When the same beam is propagated in 20 mtorr, the beam tapers more quickly, and ε_n rises during the pulse, reaching a maximum value of 1.1 rad-cm. The results are in approximate agreement with a simple analytical model which assumes free expansion at the beam head and an equilibrium pinch in the beam body.

IV. ENERGY VARIATION (DIFFERENTIAL FOCUSING) TAILORING CELL

Description of Method: This scheme involved deliberately introducing a 10-20% energy variation in the beam and passing it through a magnetic lens tuned to focus the highest energy portion in the beam body onto a scattering foil.[4] Lower energy portions are overfocused and expand before striking the foil. FRIEZR uses the thin lens approximation to model this approach.

Simulation results for differential focusing cell: Figure 6 plots the beam radius at the nominal focal point (30 cm) of a beam injected through a lens at an initial radius of 5 cm. The desired beam taper is attained, although the difference between $a_{1/2}$ and a_{rms} indicates an undesirable core-halo current density profile. The system must be tuned very accurately; a shift in the scattering foil position of only 3 cm in either direction alters the taper dramatically.

V. SUMMARY AND REFERENCES

All three conditioning techniques are capable of producing the desired radius taper although the multi-foil method may not be acceptable because of foil scattering. The IFR cell can in principle produce an excellent beam taper for stabilizing hose, but the differential focusing method is more compatible with the ATA fast corrector coil and can produce similar beam tailoring profiles if carefully tuned.

1. S. Slinker, et al., "Beam Stability and Range Extension Predictions for the ATA Multi-Pulse Experiment," these proceedings.
2. R. Adler, Part. Accel. 12, 39 (1982).
3. R. Fernsler, et al., "Foil Transport and Conditioning Cells," these proceedings.
4. W. Fawley, et al, "Conditioning Cell Design", these proceedings.
5. R. Hubbard, et al, Bull. Am. Phys. Soc. 32, 1718 (1987).

*Work supported by the Defense Advanced Research Projects Agency, ARPA Order No. 4395, Amendment 80, monitored by the Naval Surface Warfare Center.

Distribution List*

Naval Research Laboratory
4555 Overlook Avenue, S.W.

Attn: CAPT J. J. Donegan, Jr. - Code 1000
Dr. M. Lampe - Code 4792 (20 copies)
Dr. T. Coffey - Code 1001
Head, Office of Management & Admin - Code 1005
Deputy Head, Office of Management & Admin - Code 1005.1
Directives Staff, Office of Management & Admin - Code 1005.6
Director of Technical Services - Code 2000
ONR - Code 0124
NRL Historian - Code 2604
Dr. W. Ellis - Code 4000
Dr. J. Boris - Code 4040
Dr. M. Picone - Code 4040
Dr. E. Oran - Code 4040
Dr. M. Rosen - Code 4650
Dr. M. Haftel - Code 4665
Dr. S. Ossakow - Code 4700 (26 copies)
Dr. V. Patel - Code 4701
Dr. A. Robson - Code 4708
Dr. M. Friedman - Code 4732
Dr. R. Meger - Code 4750
Dr. J. Antoniades - Code 47
Dr. T. Peyser - Code 4751
Dr. D. Murphy - Code 4751
Dr. R. Pechacek - Code 4750.1
Dr. G. Cooperstein - Code 4770
Dr. A. Ali - Code 4780
Dr. D. Colombant - Code 4790
Dr. R. Fernsler - Code 4790 (20 copies)
Dr. I. Haber - Code 4790
Dr. R. F. Hubbard - Code 4790 (20 copies)
Dr. G. Joyce - Code 4790 (20 copies)
Dr. Y. Lau - Code 4790
Dr. S. P. Slinker - Code 4790 (20 copies)
Dr. P. Sprangle - Code 4790
Dr. C. M. Tang - 4790
Dr. J. Krall - Code 4790
B. Pitcher - Code 4790A
Code 4790 (20 copies)
Dr. S. Gold - Code 4793
Dr. C. Kapetanakos - Code 4795
Mr. P. Boris - SAIC (Code 5166)
Library - Code 2628 (22 copies)
D. Wilbanks - Code 2634
Code 1220

* Every name listed on distribution gets one copy except for those where extra copies are noted.

Advanced Scientific Concepts, Inc.
2441 Foothill Lane
Santa Barbara, CA 93105
Attn: Dr. Roger Stettner

Advanced Technologies Research
14900 Sweitzer Lane
Laurel, MD 20707
Attn: Mr. Daniel Weldman

The Aerospace Corporation
Mail Stop M2-269
P. O. Box 92957
Los Angeles, CA 90009
Attn: Dr. David L. McKenzie
Dr. Carl J. Rice

AFATL/DLJW
Elgin Force Base, FL 32542
Attn: MAJ Louis W. Seller, Jr.

Air Force Office of Scientific Research
Physical and Geophysical Sciences
Bolling Air Force Base
Washington, DC 20332
Attn: Major Bruce Smith

Air Force Weapons Laboratory
Kirtland Air Force Base
Albuquerque, NM 87117-6008
Attn: Dr. William L. Baker (AFWL/NTYP)
Dr. Brendan B. Godfrey
Dr. Inara Kuck

Applied Physics Laboratory
The Johns Hopkins University
Asst. to Dir. for Tech. Assessment
Johns Hopkins Road
Laurel, MD 20707
Attn: Dr. Samuel Koslov

Armed Forces Radiobiology
Research Institute
Chief, MRAD
NMC-NCR
Bethesda, MD 20814-5145
Attn: LCDR J. P. Jacobus

U. S. Army Ballistics Research Laboratory
Aberdeen Proving Ground, Maryland 21005
Attn: Dr. Donald Eccleshall (DRXBR-BM)
Dr. Anand Prakash
Dr. Clinton Hollandsworth

Avco Everett Research Laboratory
2385 Revere Beach Pkwy
Everett, Massachusetts 02149
Attn: Dr. R. Patrick
Dr. Dennis Reilly

Ballena Systems Corporation
P. O. Box 752
Alameda, CA 94501
Attn: Dr. Adrian C. Smith
Dr. William E. Wright

Ballistic Missile Def. Ad. Tech. Ctr
P.O. Box 1500
Huntsville, Alabama 35807
Attn: Dr. M. Hawie (BMDSATC-1)
Dr. M. J. Lavan (BMDATC-E)
Mr. Dan Whitener

The Boeing Aerospace Company
MS-2E30
Box 3999
Seattle, WA 98124
Attn: Dr. Robert C. Milnor

Booz, Allen, and Hamilton
Crystal Square 2, Suite 1100
1725 Jefferson Davis Highway
Arlington, VA 22202-4136
Attn: Dr. Charles M. Huddleston

Brobeck and Associates
1235 10th Street
Berkeley, CA 94710
Attn: Dr. Francis C. Younger

Chief of Naval Material
Office of Naval Technology
MAT-0712, Room 503
800 North Quincy Street
Arlington, VA 22217
Attn: Dr. Eli Zimet

Commander
Space and Naval Warfare Systems Comman
National Center 1, Room 8E08
Washington, DC 20363-5100
Attn: RADM Robert L. Topping

Cornell University
369 Upson Hall
Ithaca, NY 14853
Attn: Prof. David Hammer

Defense Advanced Research Projects Agency
1400 Wilson Blvd.
Arlington, VA 22209
Attn: Dr. H. L. Buchanan
Dr. B. Hui

Defense Nuclear Agency
Washington, DC 20305
Attn: Dr. Muhammad Owais (RAAE)
Dr. Michael Frankle
Dr. R. Gullickson

Department of Commerce
National Inst.of Standards and Tech.
Building 245, B-102
Washington, DC 20234
Attn: Dr. Mark A. D. Wilson
Dr. Steven M. Seltzer

Department of Energy
Washington, DC 20545
Attn: Dr. Wilmot Hess (ER20:GTN,
High Energy and Nuclear Physics)
Mr. Gerald J. Peters (G-256)

Department of the Navy
Chief of Naval Operations
The Pentagon
Washington,DC 20350
Attn: CAPT T. L. Sanders (OP981N3)
LCDR John Stanovich (OP981SDI)
LCDR Donald Melick (OP981SD)
Dr. Steve Bravy (OP981SDI)
Mr. Greg Montieth

Directed Technologies, Inc.
4001 Fairfax Drive, Suite 775
Arlington, VA 22203
Attn: Mr. Ira F. Kuhn
Dr. Nancy Chesser
Dr. Arthur Lee
Ms. Marla Shain

Directed Technologies, Inc.
5945 Pacific Center Blvd.
Suite 510
San Diego, CA 92121
Attn: Dr. Robert A. Jacobsen

Dr. Harald O. Dogliani
P. O. Box 503
Los Alamos, NM 87544

C. S. Draper Laboratories
555 Technology Square
Cambridge, Massachusetts 02139
Attn: Dr. E. Olsson

ESL, Inc.
Mail Stop M-4216
495 Java Drive
Sunnyvale, CA 94088
Attn: Dr. Robert A. Marth

FM Technologies, Inc.
10529B Braddock Road
Fairfax, VA 22032
Attn: Dr. F. M. Mako

GA Technologies, Inc.
P. O. Box 85608
Code 02/503
San Diego, CA 93138
Attn: Dr. Vincent Chen
Dr. Hiroyuki Ikez

General Dynamics Corporation
1745 Jefferson Davis Highway
Suite 1000
Arlington, VA 22202
Attn: Dr. Daniel W. Roth

General Dynamics Corporation
Pomona Division
1675 W. Mission Blvd.
P. O. Box 2507
Pomona, CA 92769-2507
Attn: Dr. Ken W. Hawko
Mr. C. L. Featherstone

Grumman Corporation
Grumman Aerospace Research Ctr.
Bethpage, NY 11714-3580
Attn: Dr. Richard G. Madonna

Headquarters, Department of Army
DAMOFDE, Room 2D547
The Pentagon
Washington, DC 20310-0460
Attn: LTCOL Lou Goldberg

HQ Foreign Technology Division
Wright-Patterson AFB, OH 45433
Attn: TUTD/Dr. C. Joseph Butler

HQ USAF/TXN
Patrick Air Force Base, FL 32925
Attn: CAPT Joseph Nicholas

Hudson Institute
Center for Naval Analyses
Alexandria, VA 22302
Attn: Dr. F. Bomse

Hy-Tech Research Corp.
P. O. Box 3422 FSS
Radford, VA 24143
Attn: Dr. Edward Yadlowsky

Idaho Engineering National Lab.
P. O. Box 1625
Idaho Falls, ID 83415
Attn: Dr. Francis Tsang

Institute for Defense Analyses
1801 N. Beauregard Street
Alexandria, VA 22311
Attn: Dr. Deborah Levin
Ms. M. Smith

IRT Corporation
3030 Callan Road
San Diego, CA 92121
Attn: Dr. David Phelps

JAYCOR
11011 Torreyana Road
P. O. Box 85154
San Diego, CA 92138-9259
Attn: Dr. Franklin S. Felber
Dr. Seung Kai Wong

JAYCOR
39650 Libery Street, Suite 320
Freemont, CA 94538
Attn: Dr. Kendal Casey

Joint Institute for Laboratory
Astrophysics
National Bureau of Standards and
University of Colorado
Boulder, CO 80309
Attn: Dr. Arthur V. Phelps

Kaman Sciences
P. O. Drawer QQ
Santa Barbara, CA 93102
Attn: Dr. W. Hobbs

La Jolla Institute
P. O. Box 1434
La Jolla, CA 92038
Attn: Dr. K. Brueckner

Lawrence Berkeley Laboratory
University of California
Berkeley, CA 94720
Attn: Dr. Edward P. Lee
Dr. Thomas Fessenden
Dr. William Fawley
Dr. Roger Bangerter

Lawrence Livermore National Laboratory
University of California
Livermore, California 94550
Attn: Mr. Arthur G. Cole
Dr. Michael Delong
MAJ Kenneth Dreyer
Dr. Ed Farley
Dr. Alex Glass
Dr. George Craig
Dr. C. V. Johnson, III
Dr. George Kamin
Dr. V. Kelvin Neil
Dr. Arthur C. Paul
Mr. Louis Reginato
Mr. Doyle Rogers
Dr. Dennis R. Slaughter
Dr. David Whittum
Dr. Simon S. Yu
Dr. Frank Chambers
Dr. James W.-K. Mark, L-477
Dr. William Barletta
Dr. William Sharp
Dr. John K. Boyd
Dr. John Clark
Dr. George J. Caporaso
Dr. Donald Prosnitz
Dr. John Stewart
Dr. Y. P. Chong
Dr. Hans Kruger
Dr. Thaddeus J. Orzechowski
Dr. John T. Weir
Dr. Yu-Jiuan Chen

Dr. James E. Leiss
13013 Chestnut Oak Drive
Gaithersburg, MD 20878

Lockheed Missiles and Space Co.
3251 Hanover St.
Bldg. 205, Dept 92-20
Palo Alto, CA 94304
Attn: Dr. John Siambis

Los Alamos National Laboratory
P.O. Box 1663
Los Alamos, NM 87545
Attn: Dr. L. Thode
Dr. H. Dogliani, MS-5000
Mr. R. Carlson, MS-P940
Dr. Carl Ekdahl, MS-D410
Dr. Joseph Mack
Dr. Melvin I. Buchwald
Dr. David C. Moir
Dr. Daniel S. Prono
Dr. S. Czuchlewski
Dr. Thomas P. Starke
Dr. Donald D. Cobb, D466
Dr. Robert R. Karl, D466
Dr. William B. Maier
Dr. John P. Rink
Dr. David Chamberlin

Maxwell Laboratories Inc.
8888 Balboa Avenue
San Diego, CA 92123
Attn: Dr. Ken Whitham
Dr. S. Echouse

McDonnell Douglas Research Laboratories
Dept. 223, Bldg. 33, Level 45
Box 516
St. Louis, MO 63166
Attn: Dr. Carl Leader
Dr. Frank Bieniosek
Dr. John Honig

Mission Research Corporation
1720 Randolph Road, S.E.
Albuquerque, NM 87106
Attn: Dr. Thomas Hughes
Dr. Lawrence Wright
Dr. Kenneth Struve
Dr. Michael Mostrom
Dr. Dale Welch

Mission Research Corporation
P. O. Draver 719
Santa Barbara, California 93102
Attn: Dr. C. Longmire
Dr. N. Carron

Mission Research Corporation
8560 Cinderbed Road
Suite 700
Newington, VA 22122
Attn: Dr. Khanh Nguyen

National Inst. of Standards & Tech.
Gaithersburg, Maryland 20760
Attn: Dr. Mark Wilson

National Inst. of Standards & Tech.
Radiation Physics Bldg. Room C229
Washington, DC 20234
Attn: Dr. Wayne Cassatt

National Security Agency
4928 College Avenue
College Park, MD 20740
Attn: Dr. Albert J. Leyendecker

Naval Ocean Systems Center
San Diego, CA 92152
Attn: CAPT James Fontana
Mrs. Teresita Finch
Dr. Rodney Buntzen

Naval Postgraduate School
Physics Department (Code 61)
Monterey, CA 93940
Attn: Prof. John R. Neighbours
Prof. Fred Buskirk
Prof. Kai Woehler
Prof. Xavier Maruyama

Naval Surface Warfare Center
Dahlgren, VA 22448-5000
Attn: Dr. E. M. Williams
Mr. C. E. Gallaher
Mr. Lawrence Luessen
Ms. Theresa Houghton
Dr. Ronald J. Gripshover
Dr. S. L. Moran
Dr. Edwin Ball

Naval Surface Warfare Center
White Oak Laboratory
Code R-41
Silver Spring, Maryland 20903-5000
Attn: CAPT R. P. Fuscaldo
Dr. Thomas A. Clare
CAPT R. W. Moore
Dr. Ira Blatstein
Mr. Kenneth Caudle
Mr. Carl Larson
Dr. Robert DeWitt
Dr. Ralph Schneider
Dr. Joel Miller
Dr. Stanley Stern
Dr. Omer Goktepe
Dr. A. L. Licht
Dr. Joon Choe
Mr. David Demske
Dr. Jag Sharma
Mr. W. M. Hinckley
Dr. H. S. Uhm
Dr. R. Fiorito
Dr. R. Stark
Dr. H. C. Chen
Dr. D. Rule
Dr. Matt Brown
Mrs. Carolyn Fisher (G42)
Dr. Eugene E. Nolting (H23)

Naval Technical Intelligence Center
Code DA52
4301 Suitland Road
Washington, DC 20395
Attn: Mr. Mark Chapman

New Mexico State University
Research Center
Box RC
Las Cruces, NM 88003-0001
Attn: Dr. Leon J. Radziemski

Northeastern University
Dept. of Elec. Engineering
360 Huntington Avenue
Boston, MA 02115
Attn: Dr. Philip Serafim

North Star Research Corp.
5555 Zuni, S. E.
Albuquerque, NM 87104
Attn: Dr. Richard Adler

Oak Ridge National Laboratory
Health & Safety Research Div.
P. O. Box X
Oak Ridge, TN 37830
Attn: Dr. Rufus H. Ritchie
Dr. O. Crawford

Office of the Chief of Naval Operation
Strategic and Theatre Nuclear Warfare
OP-654E4
The Pentagon
Washington, DC 20350
Attn: Dr. Yong S. Park

Office of Naval Research
800 North Quincy Street
Arlington, VA 22217
Attn: Dr. C. W. Roberson
Dr. F. Saalfeld

Office of Naval Research (2 copies)
Department of the Navy
Code 01231C
Arlington, VA 22217

Office of Under Secretary of Defense
Research and Engineering
Room 3E1034
The Pentagon
Washington, DC 20301
Attn: Dr. John MacCallum

OSWR
P. O. Box 1925
Washington, DC 20013
Attn: Dr. Jose F. Pina

PhotoMetrics, Inc.
4 Arrow Drive
Woburn, MA 01801
Attn: Dr. Irving Kofsky

Physics International, Inc.
2700 Merced Street
San Leandro, CA. 94577
Attn: Dr. E. Goldman
Dr. James Benford
Dr. George B. Frazier
Mr. Ralph Genuario

Princeton University
Plasma Physics Laboratory
Princeton, NJ 08540
Attn: Dr. Francis Perkins, Jr.

Pulse Sciences, Inc.
600 McCormack Street
San Leandro, CA 94577
Attn: Dr. Sidney Putnam
Dr. Vernon Bailey
Dr. M. Tiefenbach
Dr. J. Edighoffer
Mr. James Fockler

Pulse Sciences, Inc.
2001 Wilshire Boulevard
Suite 600
Santa Monica, CA 90403
Attn: Dr. John R. Bayless

R&D Associates
301A South West Street
Alexandria, VA 22314
Attn: Mr. Ihor Vitkovitsky
Dr. Peter Turchi

The Rand Corporation
2100 M Street, NW
Washington, DC 20037
Attn: Dr. Nikita Wells
Mr. Simon Kassel

Sandia National Laboratory
Albuquerque, NM 87115
Attn: Dr. Collins Clark
Dr. John Freeman/1241
Dr. Charles Frost
Dr. Gerald N. Hays
Dr. Michael G. Mazarakis/1272
Dr. John Wagner/1241
Dr. Ron Lipinski/1274
Dr. James Poukey
Dr. Milton J. Clauser/1261
Dr. Kenneth R. Prestwich/1240
Dr. Kevin O'Brien
Dr. Isaac R. Shokair
Dr. J. Pace VanDevender/1200
Dr. J. T. Crow
Dr. S. Shope
Dr. B. N. Turman
Dr. C. Olson
Dr. Richard Adams
Dr. Malcolm Buttram
Mr. Charles Crist
Dr. Susan Fisher
Dr. John Keizur
Dr. Gordon T. Leifeste
Dr. Raymond W. Lemke
Dr. Juan Ramirez
Dr. James Rice
Dr. Michael Wilson

Science Applications Intl. Corp.
2109 Air Park Road, S. E.
Albuquerque, NM 87106
Attn: Dr. R. Richardson
Dr. Michael D. Haworth
Dr. Alan J. Toepfer

Science Applications Intl. Corp.
5150 El Camino Road
Los Altos, CA 94022
Attn: Dr. R. R. Johnston
Dr. Leon Feinstein
Dr. Douglas Keeley
Dr. E. Roland Parkinson

University of Colorado
Dept. of Astrophysical, Planetary
& Atmospheric Sciences
Boulder, CO 80309
Attn: Dr. Scott Robertson

University of Illinois at Chicago
Dept. of Physics
P. O. Box 4348
Chicago, IL 60680
Attn: Dr. Charles K. Rhodes

University of Maryland
College Park, MD 20742
Attn: Dr. J. Goldhar
Dr. W. Destler
Dr. C. Striffler
Dr.Moon-Jhong Rhee

University of Michigan
Dept. of Nuclear Engineering
Ann Arbor, MI 48109
Attn: Prof. Terry Kammash
Prof. R. Gilgenbach

University of New Mexico
Dept. of Chem. & Nuclear Engineering
Albuquerque, NM 87131
Attn: Prof. Stanley Humphries

Commander
U. S. Army Laboratory Command
2800 Powder Mill Road
Adelphi, MD 20783-1145
Attn: George Albrecht (AMSLC-TP-PL)

U. S. Army Combined Army Center
ATZL-CAG
Ft. Leavenworth, KS 68027-5000
Attn: LTC Orville Stokes

Yale University
Mason Laboratory
New Haven, CN 06520
Attn: Dr. Ira Bernstein

Director of Research
U.S. Naval Academy
Annapolis, MD 21402 (2 copies)